Developing Magnetic Damper System for Microsatellite

Ari Legowo, Erwin Sulaeman , Muhammad Danial Rosli

Abstract— In this paper, the study of nutation damper using magnetic hysteresis is presented. There are various types of nutation damper existed and are discussed in many papers including an active nutation damper and passive nutation damper. This paper focuses only the usage of passive nutation damper because of the size limitation of microsatellite body that constraint the benefit of using active nutation control. Attitude motion of the microsatellite is described by using kinematic Euler equation where the approach of differential equation was used. The interaction of magnetic hysteresis with earth magnetic field is studied in this paper. Derivation of the governing equation in determining the attitude is briefly discussed. The effects of changing the parameter of damper characteristics as well as the effect of changing the model of the microsatellites; cylindrical and cube shape is considered. The attitude dynamics are observed by simulating the equations using MATLAB software and the results from simulation are discussed and concluded.

Keywords: advantages and disadvantages; earth magnetic field; magnetic hysteresis damper; nutation damper; SLUCUBE-2 and cylindrical model;

1. INTRODUCTION

Satellite has been widely used in aerospace mission especially in communication, relaying information, and data transmission. Meanwhile, a new technology has been introduced which is a microsatellite in 1986 [1]. The development of microsatellite has been going for over a decade. A microsatellite is a smaller satellite which benefits more in term of cost, weight and mission accomplishment [2]. Overall, it has the same aspect as a normal satellite. In space, a spinning satellite orbiting the earth is a major issue in designing the satellite and confining the movement of the satellite so that the satellite may not deviate from its path. To enable this matter, a careful mechanical design of the satellite is required and it affects the overall design of the satellite.

The attitude dynamic of a microsatellite is of primary concern in space mission for efficient operation of Earth-pointing spacecraft. The problem existed due to the perturbation of microsatellite's body over period of time and regression of orbit planes every few months [3]. Nutation of a satellite is resulted from the changing in angular acceleration of the satellite's spin motion. In space, microsatellite must be oriented such that it can accomplish the space mission [4]. External forces acting on the body of microsatellite orbiting in a low orbit tends to make the microsatellite rotates and spin around its axis [5]. Due to the motion of the Sun around the satellite's motion, spacecraft wobbling motion is observed [6]. Rotating and spinning of microsatellite are important aspects to be taken care of so that it will not deviate from the required mission. At the point when spin is adopted to stabilize a spacecraft, it is expected that the lateral angular velocity components disappear due to the gyroscopic effects [7]. Passive damping system is introduced to encounter the instability of the microsatellite. This system is used mainly to damp the frequency of nutation around its axis of rotation. Nutation dampers find general utility to maintain rotation of the body about a constant axis without perturbation [8]. Therefore, a careful modelling of nutation damper system is studied and applied in the real application.

The basic of damper is purely the work of dissipating energy and undergoes energy losses. Highly damped and pure damper mechanism differ in their precision, time taken to stop the oscillation, and how many energies dissipated. The amount of energy dissipated is a measure of the system's damping level [9]. The modelling of the damper system is benefited from the kinematic equation and the perceptive of rigid body dynamics. The dynamical equation of the satellite with the damper system is established with the aid of the equation for the first order in normal form for the rigid body. In concern of the control system, it is essential to know that the microsatellite is equipped either two types of control system; passive attitude control system (PACS) or active attitude control system (AACS) [10]. Unlike AACS, the attitude algorithm of PACS is easier and the design of the control system is made simple.

The geomagnetic field of the earth core changes corresponds to the magnetic vector of dipole axis of magnetic field [11]. The Geo-Magnetic line of forces is illustrated as in Figure 1 where the forces are originated from North Pole and travelling to South Pole. The interaction between ferromagnetic material placed in the microsatellite's body and earth magnetic field is the main contribution to the satellite attitude damping. The ferromagnetic will be induced with a flux density which is a function of the magnitude of the magnetic field and the magnetic characteristic of the material [12]. Based on Weber's theory, because of the existence of spinning atom in

Revised Manuscript Received on March 10, 2019.

Ari Legowo, Aviation Engineering Division, Higher Colleges of Technology, UAE

E Sulaeman, Department of Mechanical Engineering, International Islamic University Malaysia, Kuala Lumpur, Malaysia (Corresponding author email: esulaeman@iium.edu.my)

Muhammad Danial Rosli, Department of Mechanical Engineering, International Islamic University Malaysia, Kuala Lumpur, Malaysia

a material, the magnetic properties are possessed. The magnetic molecules existed in ferromagnetic material are aligned when magnetization occurred and such magnetic field is exists when there is an exchange interaction between electrons [13] as depicted in Figure 2. The strength of the magnetic properties of a material depends on the degree of alignment.

It is understandable that a higher degree of molecules aligned will resulted to stronger magnetic properties. The realignment of magnetic molecules induced from the earths' magnetic field will results in changing the attitude of the microsatellite.

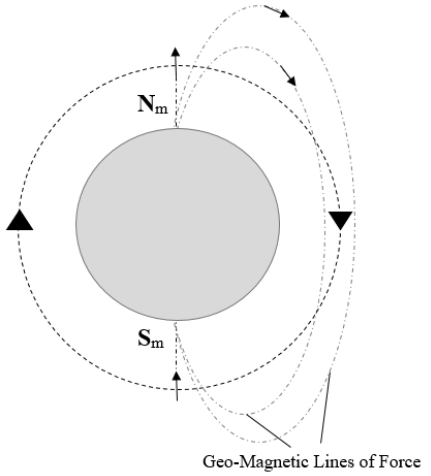

Fig. 1: An illustration of the Earth's magnetic lines of force. Nm and Sm indicate the magnetic north and south poles respectively.

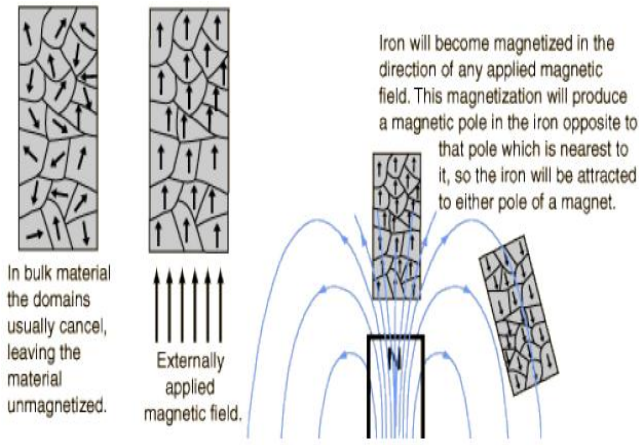

Fig. 2: Ferromagnetic molecular configuration. Retrieved December 20, 2017, from http://hyperphysics.phy-astr.gsu.edu/hbase/Solids/ferro.html.

2. MODELS OF MICROSATELLITE

In this paper, model of a cube microsatellite with dimension of 10 x 10 x 10 cm3 and weight up to 1 kg is studied. This microsatellite is the representation of SLUCUBE-2 based on previous study [14]. Another model is a cylindrical model with base diameter of 29 cm, height of 25 cm and weight of 40 kg. This paper presented the effects of hysteresis magnetic forces on the characteristics of nutation damper. Figure 3 and 4 show the 3D model for SLUCUBE-2 and cylindrical model respectively.

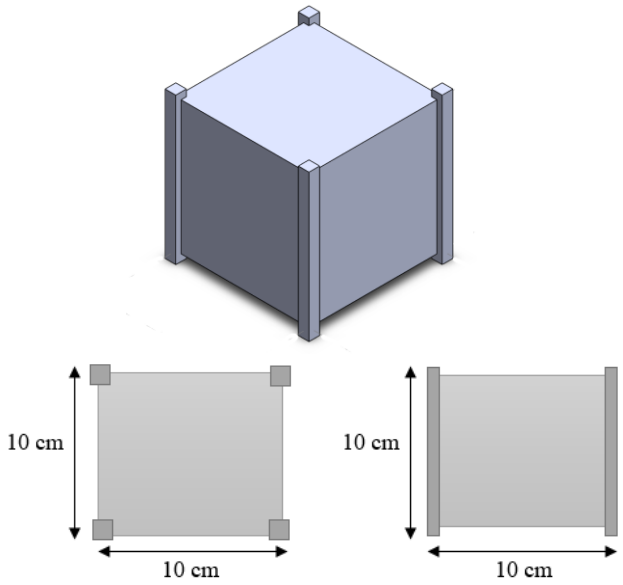

Fig. 3: Microsatellite model of SLUCUBE-2

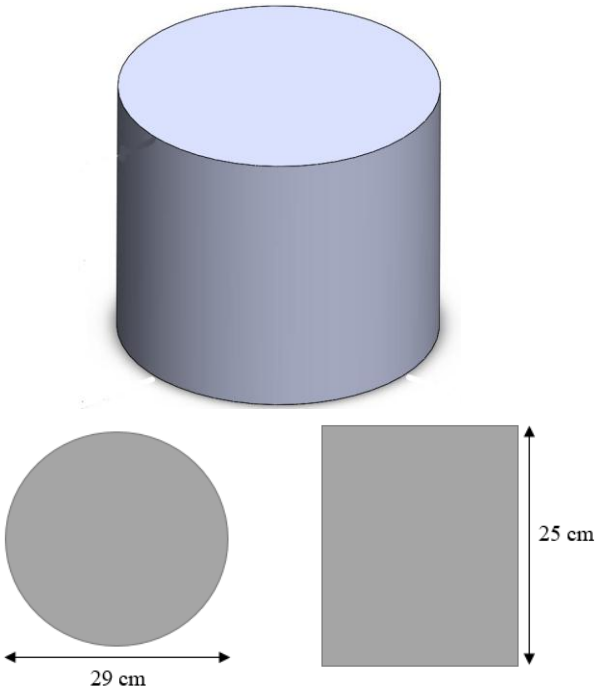

Fig. 4: Design model of cylindrical microsatellite

Since both of the models are symmetrical on its own axis and thus the body axes coincide with the pricincpal axes. In this paper, it is also assumed that the centre of mass for both models is near to the origin of principal axes. The moments of inertia for both microsatellites was calculated and are as follows:

SLUCUBE-2:

$$I_B = \begin{bmatrix} 0.00167 & 0 & 0 \\ 0 & 0.00167 & 0 \\ 0 & 0 & 0.00167 \end{bmatrix}$$

Published By:
Blue Eyes Intelligence Engineering
& Sciences Publication

Cylindrical microsatellite:

$$I_B = \begin{bmatrix} 0.42440 & 0 & 0 \\ 0 & 0.42440 & 0 \\ 0 & 0 & 0.43220 \end{bmatrix}$$

3. ATTITUDE DYNAMIC OF MAGNETIC HYSTERESIS DAMPER

In this section, dynamic equation of motions essential to observe the attitude of microsatellites are developed and derived. Numerical solutions to the differential equation observed in this chapter provide the time dependant vector of angular velocities and the change in angle (such as yaw, pitch and roll) with respect to the reference frame. The Euler's equation is derived and was used to determine the angular velocities and attitude parameters of the microsatellites.

3.1. Coordinate system

Coordinate systems were developed to derive the Euler's equation. The coordinate systems are the Inertial Reference Frame (IRF) annotated as X-Y-Z axes, Moving Referene Frame (MRF) annotated as x-y-z axes. The axes x-y-z are used to illustrate the three axis of local moving frame where the y-axis point to the direction of the microsatellite rotating the earth, z-axis pointing to the centre of the earth and x-axis completing right hand rule. Body Reference Frame (BRF) illustrated as bx-by-bz axes, such that the bx and by axis is pointed outward from plane 1 and plane 2, and bz axis is pointing outward from the top plane of the microsatellite. All three frames are true for both type of models. Figure 5(b) illustrates the coordinate frame and Figure 5(a) shows the transformation from MRF to BRF.

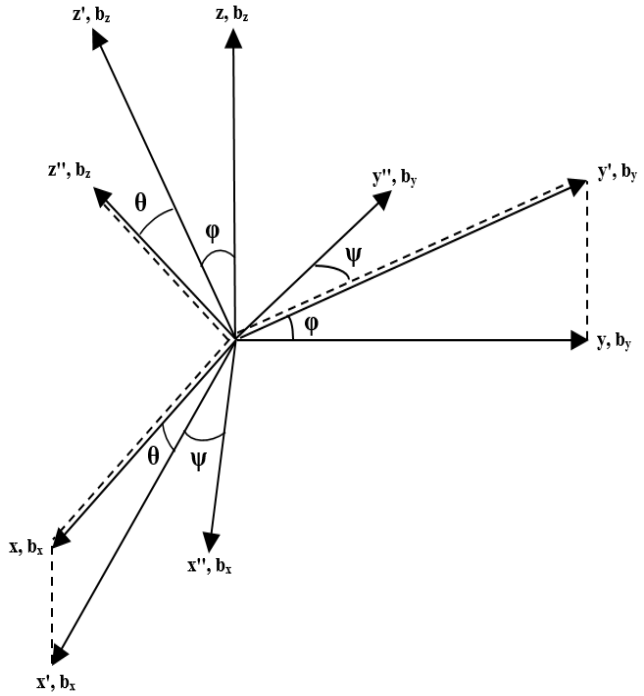

(a)

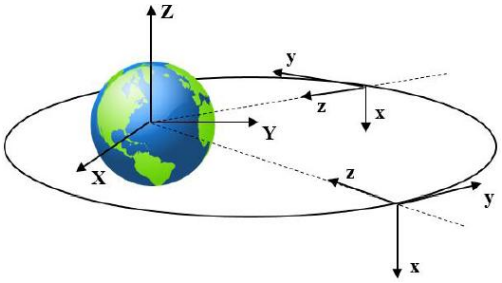

(b)

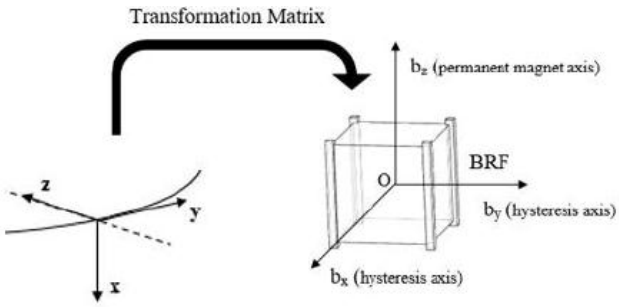

(c)

Fig. 5: (a) Transformation matrix from moving reference frame to body reference frame. (b) Coordinate system of microsatellite body with earth, (c) body reference frame.

The transformation matrix of MRF to BRF was done such that initially it assumed that b_x, b_y, and b_z axes are alligned with x, y, and z axes respectively. Firstly, the body frame is pitched along x-axis through φ angle. Then it is pitched along y'-axis with θ angle, and finally it revolved around z"-axis through ψ angle. It is represented of Euler's angle and is shown in Eq. (1). For a better understanding on the relation of the euler angles to the nutation and rotation of the microsatellite, noted that the nutation angle (also pitch angle) is revolved around y-axis and yaw angle is the microsatellite rotation along x-axis. To represent transformation from MRF to BRF, a 3x3 φ-θ-ψ transformation sequence is as follow:

$$\begin{bmatrix} b_x \\ b_y \\ b_z \end{bmatrix} = \begin{bmatrix} C_\theta C_\psi + S_\varphi S_\theta S_\psi & C_\varphi S_\psi & -S_\theta C_\psi + S_\varphi S_\theta S_\psi \\ -C_\theta S_\psi + S_\varphi S_\theta C_\psi & C_\varphi C_\psi & S_\theta S_\psi + S_\varphi C_\theta C_\psi \\ C_\varphi S_\theta & -S_\varphi & C_\varphi C_\theta \end{bmatrix} \begin{bmatrix} x \\ y \\ z \end{bmatrix} \quad (1)$$

3.2. Equation of motion

The numerical integration of the Equation of Motion (EOM) will evaluate the time history of the microsatellite's orientation. From the equation of Newtonian mechanics:

$$\boldsymbol{M} = \left(\frac{d\boldsymbol{H}}{dt}\right)_{\boldsymbol{I}} = \frac{d}{dt}\{[\boldsymbol{I}]\boldsymbol{\omega}_{\boldsymbol{B/I}}\} \quad (2)$$

In a time dependant vector $\vec{r}$ represented in two frames; body frame, $\vec{r}_B$ and inertial frame, $\vec{r}_I$,the time derivative of body frame vector is shown in Eq. (3).

$$\left(\frac{d\vec{r}_B}{dt} = -\boldsymbol{\omega}_{B/I} \times \vec{\boldsymbol{r}}_B + {}^{I}\boldsymbol{T}^{B}\frac{d\vec{r}_I}{dt}\right) \quad (3)$$

From definition, the angular momentum in the body frame can be expressed as in Eq. (4) where IB stands for mass moment of inertia in the body

Published By:
Blue Eyes Intelligence Engineering
& Sciences Publication

frame:

$$\vec{H}_B = I_B \omega_{B/I} \quad (4)$$

By making a substitution of Eq. (2) and Eq. (4) into Eq. (3), the resulting rate of angular velocity can now be expressed as in Eq. (5). (Note that $M_{ext,\,B}$ = ITB $M_{ext,\,I}$)

$$\frac{d\omega_{B/I}}{dt} = I_B{}^{-1}\{M_{ext,B} - \omega_{B/I} \times (I_B \cdot \omega_{B/I})\} \quad (5)$$

In this paper, it is assumed that the microsatellite is orbiting the earth with constant speed in a circular orbit. Thus, the mean motion (***n)*** of the microsatellite is stated as in Eq. (6) (where a is the orbital radius and μ is the Earth Gravitation Parameter, μ = 3.986 x 10^5 $km^3.s^{-2}$)

$$n = \sqrt{\frac{\mu}{a_{orb}{}^3}} \quad (6)$$

The angular velocity of the moving reference frame with respect to the inertial reference frame can be annotated as Eq. (7) where this equation is expressed in body frame with unit vector of y axis (take note that this equation is using the transformation matrix of body frame from moving reference frame).

$$\omega_{M/I} = -n({}^M T^B)\begin{bmatrix}0\\1\\0\end{bmatrix} \quad (7)$$

The negative sign annotated above shows that the microsatellite's orbiting angular velocity is opposite to the local rotating frame's y-axis. Thus the angular velocity of body frame relative to the local rotating frame can be expressed as in Eq. (8).

$$\omega_{B/M} = \omega_x \hat{b}_x + \omega_y \hat{b}_y + \omega_z \hat{b}_z \quad (8)$$

Substitute Eq. (7) into Eq. (8), it can get a new expression of the angular velocity at the body frame which in the later used to derived the change in the Euler angles. The expression of angular velocity at the body frame is shown in Eq. (9).

$$\begin{bmatrix}\omega_x\\ \omega_y\\ \omega_z\end{bmatrix} = \omega_{B/I} + n({}^M T^B)\begin{bmatrix}0\\1\\0\end{bmatrix} \quad (9)$$

By using the transformation matrix expressed in Eq. (1), the Euler angles rate obtained from Eq. (9) are as follows:

$$\frac{d\theta}{dt} = \frac{1}{cos\varphi}[\omega_x sin\psi + \omega_y cos\psi]$$

$$\frac{d\varphi}{dt} = [\omega_x cos\psi - \omega_y sin\psi] \quad (10)$$

$$\frac{d\psi}{dt} = tan\varphi[\omega_x sin + \omega_y cos\psi] + \omega_z$$

By getting the angular velocity of the body frame related to the inertial frame from Eq. (5) from each time step, Eq. (9) is used to get the angular velocity of the body frame to be used in Eq. (10) to obtain the Euler angle at each time step. From this iteration, it can be seen that all these three equations are essential to each other to get the Euler angles at each time step. These three equations are the governing equations to be taken care of in the simulation.

3.3. Magnetic and hysteresis torque modelling

To obtain the external magnetic forces as in this case the Earth magnetic field, International Geomagnetic Reference Field (IGRF) provides a sufficient data on the magnetic field of the earth as. IGRF expresses the magnitude of magnetic field as a function of Earth's longitude and latitude. Once the IGRF is updated using new data, it is called Definitive Geomagnetic Reference Field (DGRF) [15]. The quantum mechanics of earth's magnetic field is quite ambitious and it is not the focused in this paper. To get the scalar values of the Earth's magnetic line forces, the DGRF/IGRF (Definitive Geomagnetic Reference Field) provides sufficient data with reasonable view of latitude and longitude of the earth.

By knowing the magnet's rated magnetic induction B (Tesla), the volume of the magnet $V(m^3)$, and the permeability of free space $\mu_o = 4\Pi \times 10^{-7}$ N/A^2, and the axis of dipole moment (positive $\mathbf{b_2}$ **axis)** the dipole moment vector of the permanent magnet is expressed in Eq. (11).

$$\vec{\mu}_B = \frac{B.V}{\mu_0}\begin{bmatrix}0\\1\\0\end{bmatrix} \quad (11)$$

From the DGRF/IGRF model, the magnetic field vector $\vec{B}$ (Tesla) can be determined. Thus the cross product of $\vec{B}$ and $\vec{\mu}_B$ will result the external moment exerted by the permanent magnet. It is shown in Eq. (12) where the external torque to be determined at a given point in the orbit.

$$M_{perm.B} = \vec{\mu}_B \times \vec{B}_B \quad (12)$$

After knowing the permanent magnet torque, the equation of hysteresis damper is derived. The equation governing the behaviour of the hysteresis magnet is expressed in Eq. (13). The hysteresis loop as depicted in [14, Fig 6] shows the magnetic induced from external magnetic field which Eq. (13) dynamically predicts. Some important parameters are the saturation induction (maximum magnetization) Bm, the residual magnetic forces Bo and the coercive force Ho. Some papers may annotate these parameters as Bs, Br and Hc respectively. These three parameters are of important aspect of a hysteresis magnet that define its behaviour.

At a neutral point where no external magnetic forces existed, the material will have the original magnetic field at point Ho and Bo. When an external forces exerted in a positive direction (to the right), the magnetic field (H) and flux density (B) increased until they reach saturation induction (Bm) where the magnet has maximum magnetization. The same cases applied when another external forces exerted on the magnetic field in opposite direction (to the left). The differences in earth's magnetic field affect the hysteresis loop of the magnetic material installed in the microsatellite.

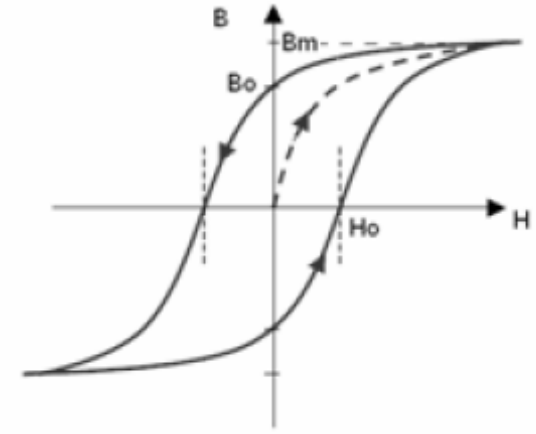

Fig. 6: Hysteresis loop diagram. Adapted from [14]

The dynamic induction of the magnetic forces depending on the external magnetic field can be used to compute the corresponding damping moment Mhys, B by using Eq. (11) and Eq. (12) knowing the volume of hysteresis material (with unit vector on b1 or b3axis) and the external magnetic field.

$$\boldsymbol{B} = \frac{2B_m}{\pi} tan^{-1}\left[\frac{1}{H_0} tan\left(\frac{\pi B_0}{2B_m}\right)(\boldsymbol{H} \pm \boldsymbol{H_0})\right] \quad (13)$$

4.SIMULATION METHOD, RESULT AND DISCUSSION

In this paper, the software used to simulate all the attitude dynamics for both systems is using MATLAB. Before the hysteresis magnet is analysed, a free torque motion is first simulated to perceive the behaviour of microsatellite's body. From Eq. (2) the value of external moment will be zero.

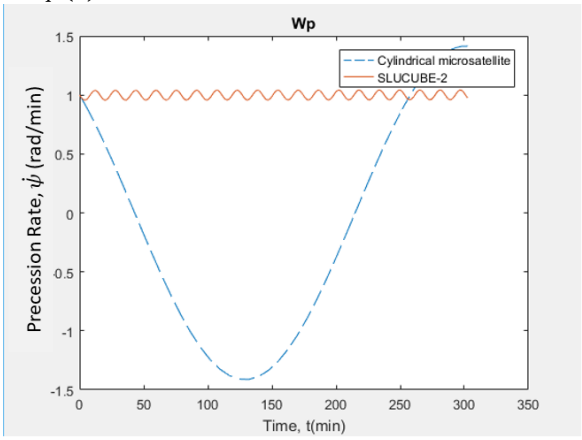

(a)

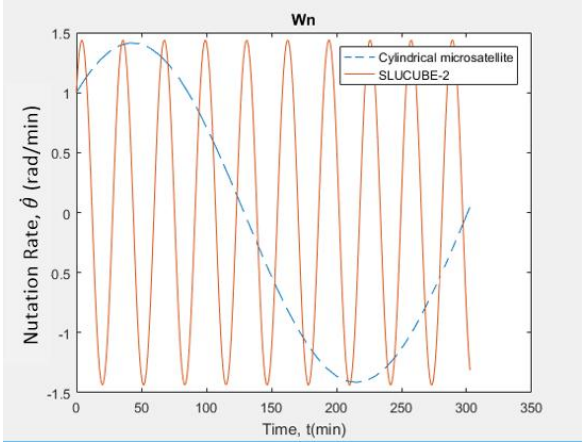

(b)

Fig. 7: Comparison of attitude dynamic between cylindrical microsatellite and SLUCUBE-2 on a free torque environment. (a) Precession rate (b) Nutation rate

The imbalance existed in a spinning rigid body can be in the form of static or dynamic imbalance. From Figure 7, it can be seen that both models wobble on the nutation and precession angle. Although both models did not dynamically balance but it is safe to say that they are statically stable because there are no divergences existed in the motion.

Now that the free torque motion is analysed, the effects of putting permanent magnet and hysteresis magnet are studied. In this analysis, the microsatellite is first assumed to have only permanent magnet attached on the $\mathbf{b}_y$ axis where the dipole moment of the permanent magnet is aligned with the earth's magnetic field. The earth's magnetic field can be obtained from the DGRF/IGRF website as previously stated. Using the DGRF/IGRF data, the interaction of permanent magnet and hysteresis magnet with the external magnetic field can be calculated using Eq. (13) corresponding to each type of magnet. With permanent magnet induction rated with B = 3.6 Tesla and hysteresis magnet (PERMENORM 500 H2) characteristics are Bo = 0.012 Tesla, Bm = 0.25 Tesla, Ho = 0.035 Oe, Volume = 3.75×10^{-7} m^3.

The simulation method used for hysteresis magnetic damper is to solve Eq. (5), Eq. (9), Eq. (10) for each time step taking into consideration the external torque produced by the magnet with the initial conditions; Euler angles are zero (assumed the body frame is aligned with local moving frame) and angular velocity is 1 rad/s (assumed a slight perturbation from external forces such as solar radiation and gravity). The microsatellites are assumed to orbit in circular at a constant speed in Low Earth Orbit (LEO) of altitude 800 kilometres. It is calculated that it takes approximately 100 minutes to complete one orbit. Thus, the time span used in the simulation can be viewed as 100 minutes per orbit.

The hysteresis magnet is placed parallel to the bx or by axis; usually orthogonal to axis of the permanent magnet. It can be seen that the yaw angle and the pitch angle are damped. It is because the torque produce by the permanent magnet loses energy due to the hysteresis magnet. The hysteresis magnet realigns the dipole moment as discussed in the literature review. Pertinent to this fact, it can be said that to optimize the permanent magnet, the hysteresis magnet is essential to the system and the hysteresis damper system is feasible. Figure 8(a) showing that the yaw angle, φ did not reach 90 degrees. Thus from Eq. (10) the equation does not have singularity, which validate the sequence of transformation matrix chosen. It is safe to say that it validates the choice of transformation sequence of φ – θ – ψ.

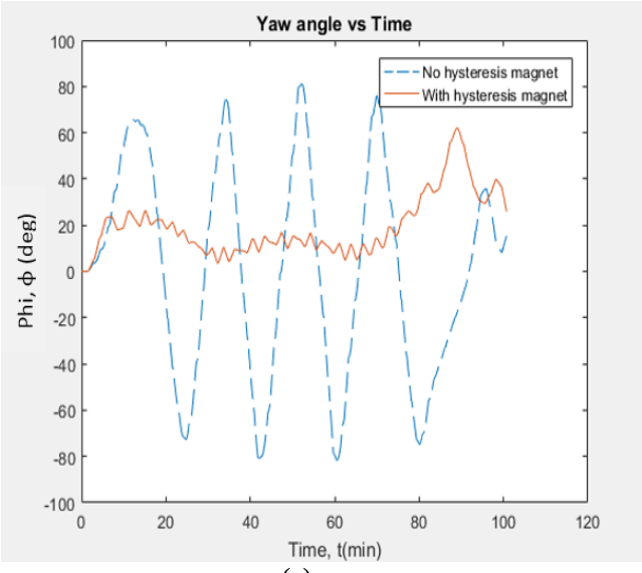

(a)

Published By:
Blue Eyes Intelligence Engineering
& Sciences Publication

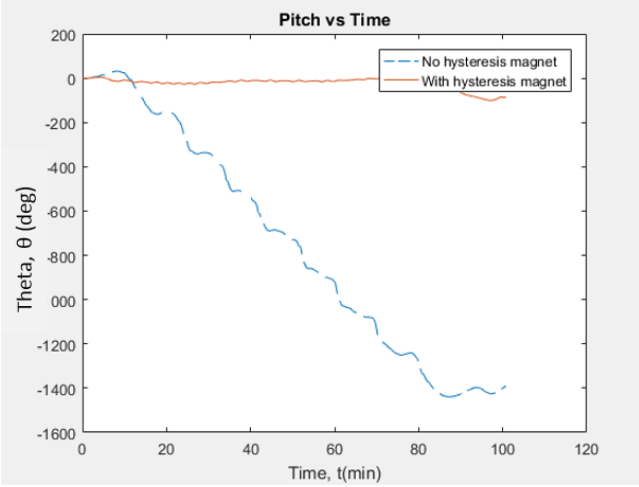

(b)

Fig. 8: Change in yaw and pitch angle of SLUCUBE-2 with (solid line) and without hysteresis magnet (dash line). (a) Yaw angle (b) Pitch angle

Then for the effect of changing the parameters of the damper system to the attitude dynamic of the microsatellite, Figure 9 illustrates the comparison of two different volume of hysteresis magnet. From the graph, it can be seen that bigger hysteresis magnet which is 3.9 x 10-7 m3 depicted with dotted line will tolerates more energy losses. Of course, a stable yawing angle contributes to a stable pitch angle. Thus, it is good to say that a bigger hysteresis magnet used contributes to nutation stability.

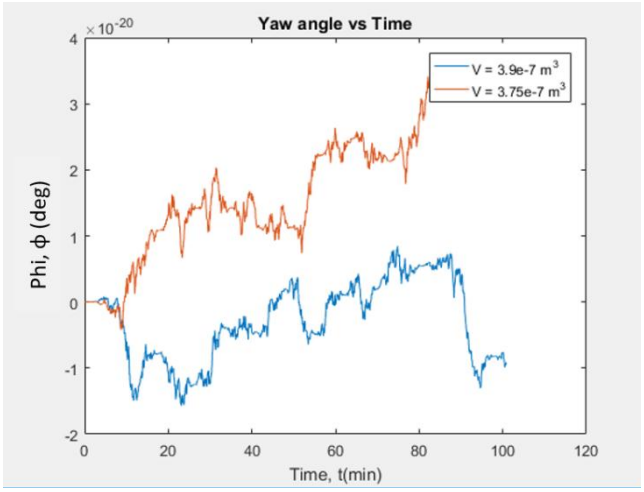

Fig. 9: Comparison of the effect of different volume of hysteresis magnet on the microsatellite motion.

Now, the model is changed to the cylindrical microsatellite and the attitude dynamic is observed. The moment of inertia for the cylindrical microsatellite was stated in the previous chapter. The attitude dynamic of the cylindrical microsatellite by using the magnetic hysteresis damper is depicted in the graphs as in Figure 10. It can be seen that the graphs are smoother and more stable compared to using SLUCUBE-2 model. However, while the system is achieving the stability, it cannot be neglected that the motion is not damped fully. As per se, the cylindrical microsatellite needs a bigger volume of hysteresis magnet or in other word the bigger the size of the spacecraft the bigger the size of the hysteresis magnet should be. It is true to the fact that a bigger size of rigid body, more energy needed to dissipate for the stability of the microsatellite, which in this case a bigger size of hysteresis magnet compliment to this theory. Noted that changing the parameter of the hysteresis magnet will result the same outcome as in SLUCUBE-2.

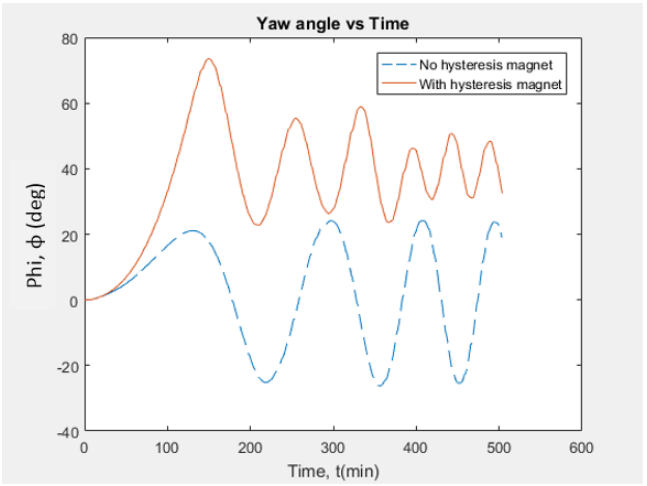

(a)

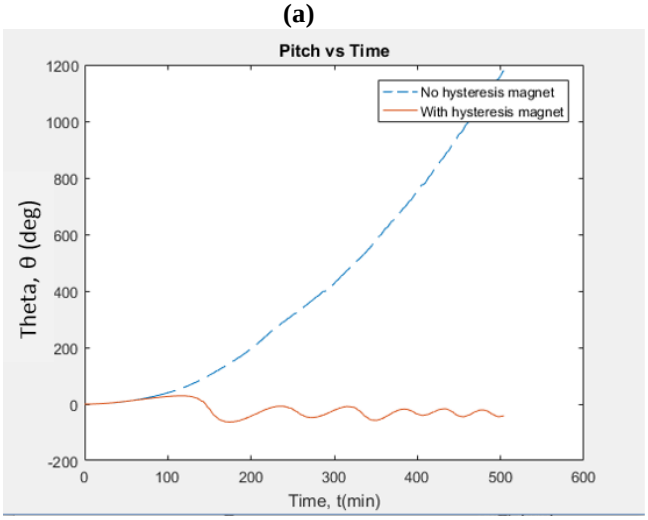

(b)

Fig. 10: The change in yaw and pitch angle of cylindrical microsatellite with (solid line) and without damper (dash line). (a) Yaw angle (b) Pitch angle

5. CONCLUSION

Taking everything into consideration, due to the limitations exist in the development of microsatellite, the approach of passive means of magnetic damping is preferred. The limitations are the size of the microsatellite, the desired weight of the microsatellite and its controllability. Using hysteresis magnetic damper showed a promising way of damping the nutation of the microsatellite as well as its rotation. However, the drawbacks of using this system it is not suitable for a big and heavy spacecraft. The interaction of hysteresis magnet and earth's magnetic field is weak to damp the microsatellite's wobbling motion. Therefore, the energy dissipation in this system is small and it can be said that this system is only suitable for lighter and smaller microsatellites. Nonetheless, the approach of magnetic hysteresis damper is preferable because of it effortless in deriving the equation and installing the damper system into the microsatellite.

Further continuation of this project must be done to do the actual test and compare with the simulation result. Moreover, the approach of using quaternion method is preferable due to its robustness and faster.

Appendix A: Nomenclature

H_B = angular momentum in the body frame
$M_{ext,B}$ = external moment
I = Moment of Inertia
I_B = mass moment of inertia
$\omega_x, \omega_y, \omega_z$ = angular velocity at the moving frame
b_x, b_y, b_z = angular velocity at the body frame
θ, φ, ψ = pitch, roll and yaw angle respectively
$\omega_{B/I}$ = Angular Velocity of Body Frame Related to Inertial Frame
$\omega_{B/M}$ = Angular Velocity of Body Frame Related to Rotational Frame
$\omega_{M/I}$ = Angular Velocity of Rotational Frame Related to Inertial Frame
n = Mean Motion of Microsatellite
μ = Geocentric gravitational constant (398 600 km^3/sec^2)
B = Earth's magnetic flux
$\vec{B}_B$ = magnetic field vector
Bm = saturation induction
Bo = residual magnetic force
Ho = coercive force
B_h = Magnetic flux induced in the hysteresis rod
V_h = Volume of hysteresis rod
μ_0 = Permeability of free space
μ_B = Dipole moment vector of permanent magnet
a_{orb} = Orbital Radius
${}^{M}T^{B}$ = Transformation matrix of MRF to BRF

ACKNOWLEDGEMENT

The support of Malaysian Ministry of Education through Intertional Islamic University Malaysia under the research grant FRGS17-036-0602 is gratefully acknowledged.

REFERENCES

1. S. W. Janson (2011) "25 Years of Small Satellites" 25th Annual AIAA/USU Conference on Small Satellites, Utah State University.
2. I. Nikolova (2005) "Microsatellites Advantages, Profitability and Return" in Space, Ecology, Safety, Varna, Bulgaria.
3. H. Hablani (1995) "Magnetic precession and product-of-inertia nutation damping of bias momentum satellites" vol. 18.
4. B. M. Menges, C. A. Guadiamos, and E. K. Lewis (1998) "Dynamic Modeling of Micro-Satellite Spartnik's Attitude" IEPC Pap., pp. 1–17.
5. V. V Lyubimov and S. V Podkletnova (2016) "Modeling the optimal reduction of the small angular velocity of a microsatellite using onboard magnetic coils" in 2016 Dynamics of Systems, Mechanisms and Machines (Dynamics) pp. 1–5.
6. D. Kucharski et al. (2016) "Confirmation of gravitationally induced attitude drift of spinning satellite Ajisai with Graz high repetition rate SLR data"Adv. Sp. Res.
7. D. Yang, Y. Xiong, Q. Ren, and X. WANG (2017) "Nutation instability of spinning solid rocket motor spacecraft" Chinese J. Aeronautics.
8. J. Evans, Nutation damper. United States Patent US3737118A, 1973.
9. Libii, J.N (2009) "Demonstration of Energy Dissipation in a Spring-Mass System Undergoing Free Oscillations in Air" World Transaction on Engineering and Technology Education, vol. 7, pp. 28-33.
10. M. Ovchinnikov (1999) "Methods to Control the Attitude Motion of a Satellite by the Earth's Magnetic Field Usage" Coop. Space, Euro-Asian Sp. Week where East West Final. meeting, Singapore, 23-27 Novemb. 1998. Paris Eur. Sp. Agency (ESA), ESA-SP Vol. 430, 1999. ISBN 9290927208, p.475, vol. 430, pp. 475–483.
11. G. Hulot, C. C. Finlay, C. G. Constable, N. Olsen, and M. Mandea, (2010) "The magnetic field of planet earth" Space Sci. Rev.
12. G. Bertotti (1998) Chapter 1 - Magnetic Hysteresis, in Electromagnetism, G. B. T.-H. in M. Bertotti, Ed. San Diego: Academic Press, pp. 3–30.
13. Y. Mnyukh (2012) "Ferromagnetic State and Phase Transition" American Journal of Condensed Matter Physics 2(5), 109-115.
14. Sanjay Jayaram and Darren Pais (2012) "Model-based Simulation of Passive Attitude Control of SLUCUBE-2 Using Nonlinear Hysteresis and Geomagnetic Models" Int. J. Aerosp. Sci., vol. 1, no. 4, pp. 77–84.
15. J. Gianibelli, K. Jacqueline, and M. Ghidella (2003) "Testing Geomagnetic Reference Field models for 1990-2000 with data from the Trelew Geomagnetic Observatory", Argentina, vol. 42.

Published By:
Blue Eyes Intelligence Engineering
& Sciences Publication